Slope Winds and the Axisymmetric Circulation over Antarctica

J. EGGER

Meteorologisches Institut der Universität München, München, FRG

(Manuscript received 20 December 1984, in final form 24 April 1985)

ABSTRACT

An axisymmetric model of the flow over Antarctica is used to study the circulation induced by cooling of the air at the slopes of the continent. It is found that the resulting circulation with southeasterly surface winds and westerlies in the free troposphere agrees qualitatively quite well with the observed circulation. The profiles of wind and temperature obtained above the slope are compared to the results from a simple one-dimensional model of flow over sloping terrain. The agreement is quite good near the surface but not at upper levels. The reasons for this discrepancy are discussed. It is found that the two-dimensional flow does not settle down to a satisfactory steady state. It is argued that the surface easterlies at the slopes of Antarctica provide a source of westerly angular momentum. In the atmosphere, three-dimensional eddies can export momentum to lower latitudes, whereas the flow in the model cannot dispose of the momentum. This points to the limitations of the two-dimensional approach.

1. Introduction

Although the orography of Antarctica cannot be called axisymmetric with the Ross Sea and the Wedell Sea penetrating deeply into the continent and the highest elevations being off the South Pole by a few hundred kilometers, the overall shape of Antarctica is nevertheless strongly reminiscent of a cone with rather gentle slopes. This near axisymmetry is reflected in the time-mean circulation over Antarctica. Close to the ground we have a quite pronounced axisymmetry of the flow towards the coast (Mather and Miller, 1967; Schwerdtfeger, 1970, Fig. 25) which is distorted somewhat by the more prominent orographic features of Antarctica. Aloft there is an almost circular cyclonic circulation throughout the year with the pressure minimum slightly off the South Pole (van Loon, 1972). Again the axisymmetry is distinct but not perfect. This suggests that an axisymmetric theory of the Antarctic circulation is not hopeless *a priori*. Correspondingly, an attempt is made in this paper to develop an axisymmetric flow model and to see if one can explain at least some of the most basic axisymmetric features of the Antarctic circulation. To achieve this goal one has to isolate the most important driving mechanisms. Roughly speaking, the Antarctic circulation is driven by radiative processes, by the interaction with the sloping cold ground and by the interaction with the flow at mid-latitudes. Comprehensive modeling of all these driving mechanisms requires, of course, a general circulation model. In fact, the circulation of Antarctica has been studied several times within the framework of simulations of the general circulation of the atmosphere by aid of GCMs (e.g., Hermann and Johnson, 1980; see also JOC, 1979, for a documentation of relevant work).

In these numerical experiments all driving mechanisms are acting simultaneously and it is, therefore, difficult to isolate cause and effect. Here a less ambitious approach will be chosen. We select the interaction of the air with the cold sloping ground as one important driving mechanism and ask what type of circulation is set up by this process. In this way we hope to achieve a better understanding of the impact of the conditions at the lower boundary on the Antarctic circulation. We are not aware that papers on this problem have been published yet. However, the slope winds in Antarctica as one aspect of this problem have attracted some interest and it is perhaps fair to say that the most basic features of the wind profiles in the boundary layer are understood reasonably well (Ball, 1960; Lykosov and Gutman, 1972). On the other hand, these theoretically determined slope winds do not satisfy the balance of mass for the Antarctic circulation since there is a vertically averaged mean flow down the slope. A flow model for the Antarctic circulation has to take into account the return flow aloft. This can be done in a model which is two-dimensional. Quite recently, Parish (1984) published results obtained from three-dimensional numerical experiments designed to simulate strong katabatic flows near the coast. Since the domain of integration covers only a small part of the continent, Parish did not address the problem of the mean circulation of Antarctica.

In Section 2 we present a two-dimensional axisymmetric model. Section 3 is devoted to a discussion of one-dimensional theories of slope winds. The results from the two-dimensional model are described in Section 4 and compared to the results obtained from the one-dimensional models. Critical remarks will be found in Section 5.

2. The model

Consider an axisymmetric flow domain as depicted in Fig. 1. Its boundaries are the earth's axis to the south and a solid wall to the north of Antarctica. At the lower boundary we have the slopes of the continent and the sea to the north. On top, an interface is assumed with a motionless fluid of constant density ρ_1 above. We adopt axisymmetric coordinates (r, z). We want to study the problem of what type of flow is excited in the flow domain if we prescribe low temperatures at the slopes. We exclude three-dimensional eddies from our consideration so that we can immediately write the equations for axisymmetric Boussinesq flow:

$$\frac{du}{dt} = -\frac{vu}{r} + fv + K\frac{\partial^2 u}{\partial z^2} \tag{2.1}$$

$$\frac{dv}{dt} = \frac{u^2}{r} - fu - \frac{1}{\rho_0}\frac{\partial p}{\partial r} + K\frac{\partial^2 v}{\partial z^2} \tag{2.2}$$

$$\frac{1}{\rho_0}\frac{\partial p}{\partial z} = g\frac{\theta}{\theta_0} \tag{2.3}$$

with

$$\frac{d}{dt} = \frac{\partial}{\partial t} + \frac{1}{r}\frac{\partial vr}{\partial r} + \frac{1}{\rho_0}\frac{\partial}{\partial z}w\rho_0$$

$$\frac{d\theta}{dt} + \frac{d\theta_0}{dz}w = -\delta\theta + K\frac{\partial^2\theta}{\partial z^2} \tag{2.4}$$

$$\frac{1}{\rho_0}\frac{\partial}{\partial z}(w\rho_0) + \frac{1}{r}\frac{\partial}{\partial r}(rv) = 0 \tag{2.5}$$

$$\frac{\partial\eta}{\partial t} + \frac{1}{r}\frac{\partial vr\eta}{\partial r} = w_{H_0+\eta} \tag{2.6}$$

where v is the downslope component of velocity, u the zonal component and w represents the velocity in the vertical (see Fig. 1); η is the deviation of height of the free surface from a mean height H_0 and $\theta(p)$ is the deviation of potential temperature (pressure) from the potential temperature $\theta_0(z)$ [pressure $p_0(z)$] of the basic state. This basic state (subscript 0) is assumed to be motionless and time independent. Density and potential temperature of the basic state are derived from the prescribed polytropic profile of temperature

$$T_0(z) = T_{00} - \hat{\gamma}z \tag{2.7}$$

with lapse rate $\hat{\gamma}$. The stability of the basic state is characterized by the Brunt–Väisälä frequency

$$N_0^2 = \frac{g}{\theta_0}\frac{d\theta_0}{dz}. \tag{2.8}$$

The concept of a background state appears to be well suited to our purpose. After all, the circulation induced by the cooling at the surface is only one part of the Antarctic flow and we cannot hope to simulate realistic stabilities in a model which excludes important driving mechanisms. By prescribing the basic state we essentially assume that this background state is maintained by all the other forcing mechanisms excluded in our work. Turbulent mixing in the vertical is included rather crudely using a K-ansatz with constant K. In (2.4) we have a radiative damping term with damping time δ^{-1}. Note that f is negative in (2.1), (2.2). We adopt a value of the Coriolis parameter which corresponds to 70°S. The boundary conditions are as follows. Over land we have $\theta = \theta_s < 0$ at the ground and $\theta = 0$ at the sea surface. We require $u = v = w = 0$ at all boundaries except at the interface where no stress conditions $\partial u/\partial z = \partial v/\partial z = 0$ are imposed. The upper boundary condition (2.6) is virtually equivalent to that used in σ-coordinate models (e.g., Kasahara, 1974).

We solve (2.1)–(2.6) by numerical means. The equations are solved in a grid. The staggering of the variables in the grid is shown in Fig. 1. In particular we replace the slope of Antarctica by a step profile. Centered differences are used in space and time except in (2.6) where the advective terms are treated according to the "donor cell" method (e.g., Roache, 1976).

The treatment of the upper boundary is somewhat problematic. In order to implement (2.6) without any approximations we would have to use a σ-coordinate system which follows the interface. We avoid the complications inherent in this approach by using a grid which is fixed in space. The uppermost computational level of this grid is at $z = H_0$. We solve (2.6) at $z = H_0$ and not at $z = H_0 + \eta$. The height of the free surface is predicted this way and enters the problem when the hydrostatic equation (2.3) is integrated vertically. Then we specify the pressure at $z = H_0$:

$$p(H_0) = g'\rho_0(H_0)\eta \tag{2.9}$$

where $g' = (\rho_0(H_0) - \rho_1)g/\rho_0(H_0)$ is a reduced gravity. With (2.9), (2.3) is integrated downward from the level $z = H_0$. All these approximations are certainly acceptable as long as η is small. We defer a discussion of this problem until later. We use a horizontal grid spacing of $\Delta r = 50$ km and a time step $\Delta t = 200$ s in our leap frog scheme. In the vertical we apply a coordinate stretching. We have $\Delta z = 150$ m near the ground. This

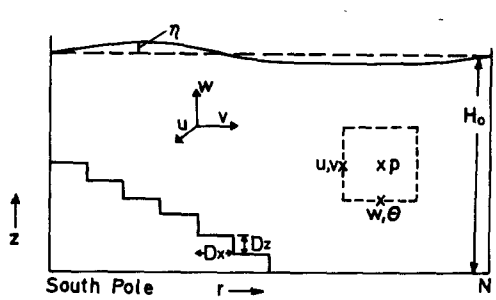

FIG. 1. Domain of integration and the grid of the model. See text for further explanation.

resolution extends up to a height $H_n \sim 3700$ m well above the uppermost plateau of Antarctica. Above that height we apply a linear stretching of Δz so that $\Delta z = 300$ m above a height of 5500 m. The free surface is at a height $H_0 = 7500$ m.

3. One-dimensional slope winds

Before presenting the numerical results we think it helpful to discuss first the one-dimensional case where an analytic solution of the problem is feasible. We extend here the work of Lykosov and Gutman (1972). These authors looked at the flow along a slope with an angle of inclination γ in a rotating system. It is assumed that the slope is infinitely extended. This means that we have to abandon the circular geometry used so far, thus replacing r by a Cartesian coordinate y. We choose a coordinate system where the y-axis is parallel to the slope, the x-axis is parallel to the heightlines of the terrain and the z-axis is perpendicular to the slope (Fig. 2). For the sake of simplicity we do not introduce a separate notation for this new system. Because of the slope's infinite extent we can assume that all derivatives with respect to y vanish. It follows from the equation of continuity that $w = 0$ where w is the velocity perpendicular to the slope. Then, (2.1), (2.2) and (2.4) become in the new coordinate system

$$-fv\cos\gamma = K\frac{\partial^2 u}{\partial z^2} \tag{3.1}$$

$$fu\cos\gamma = -\frac{g\theta}{\theta_0}\sin\gamma + fu_g\cos\gamma + K\frac{\partial^2 v}{\partial z^2} \tag{3.2}$$

$$-\frac{N_0^2}{g}v\sin\gamma = \frac{K}{\theta_0}\frac{\partial^2\theta}{\partial z^2} - \frac{\delta\theta}{\theta_0} \tag{3.3}$$

where we assume that neither θ_0 nor N_0^2 depend on height and where stationarity has been imposed. When writing down (3.1)–(3.3) we have assumed that $\gamma \ll |\varphi|$ (φ latitude),—an assumption that is certainly justified in Antarctica. The simplest case treated by Lykosov and Gutman (1972) is close to (3.1)–(3.3) except that the radiative damping term is excluded. On the right hand side of (3.2) we have added a pressure gradient term $fu_g\cos\gamma$. Boundary conditions are: $u = v = 0$, $\theta = \theta_s < 0$ at $z = 0$ and $v = \theta = 0$, $u = u_g$ at infinity. As has been pointed out by Lykosov and Gutman (1972), such a geostrophic wind is needed if a stationary solution is to exist for $\delta = 0$. This can be shown by combining (3.1) and (3.3) with $\delta = 0$:

$$\frac{\partial^2}{\partial z^2}\left(u - \frac{fg\cos\gamma\theta}{\theta_0 N_0^2\sin\gamma}\right) = 0. \tag{3.4}$$

An integration with respect to z yields

$$\frac{\partial u}{\partial z} - \frac{fg\cos\gamma}{\theta_0 N_0^2\sin\gamma}\frac{\partial\theta}{\partial z} = 0. \tag{3.5}$$

In (3.5) the constant of integration had to vanish because $\partial u/\partial z = \partial\theta/\partial z = 0$ at infinity. Equation (3.5) states that the turbulent transport of heat must be balanced by a turbulent transport of zonal momentum. Now if (3.5) is integrated again over z taking into account the conditions at the surface we have

$$u - \frac{fg\cos\gamma\theta}{\theta_0 N_0^2\sin\gamma} = -\frac{fg\cos\gamma\theta_s}{\theta_0 N_0^2\sin\gamma} \tag{3.6}$$

and, therefore,

$$u_g = -\frac{fg\cos\gamma\theta_s}{\theta_0 N_0^2\sin\gamma} \tag{3.7}$$

so that we have an easterly geostrophic wind ($f < 0$, $\theta_s < 0$) aloft. Of course, these geostrophic easterlies are unrealistic.

To solve (3.1)–(3.3) with radiative damping included we eliminate variables and arrive at a sixth-order differential equation

$$\left(\frac{\partial^6}{\partial z^6} - \frac{\delta}{K}\frac{\partial^4}{\partial z^4} + 4\lambda^4\frac{\partial^2}{\partial z^2} - \delta f^2\cos^2\gamma/K^3\right)\begin{pmatrix}\tilde{u}\\ v\\ \theta\end{pmatrix} = 0 \tag{3.8}$$

where

$$4\lambda^4 = (f^2\cos^2\gamma + N_0^2\sin^2\gamma)/K^2 \tag{3.9}$$

and $\tilde{u} = u - u_g$. It is instructive to consider first the case $\delta = 0$. With $\delta = 0$ the solutions of (3.8) are of the form $\exp(-\lambda z)(A\cos\lambda z + \sin\lambda z)$. In particular, the potential temperature

$$\theta = \theta_s\cos\lambda z\exp(-\lambda z) \tag{3.10}$$

increases above the slope and we have $\theta = 0$ at the height $\pi/2\lambda$. The slope wind

$$v = -(2\lambda^2\theta_s Kg/\theta_0 N_0^2\sin\gamma)\exp(-\lambda z)\sin\lambda z \tag{3.11}$$

blows down the slope for $\theta_s < 0$ with a maximum at the height $\pi/4\lambda$. The slope wind layer has a thickness π/λ with a relatively weak return flow above that layer. Note that

$$\int_0^\infty v dz = -\theta_s g K\lambda/\theta_0 N_0^2\sin\gamma > 0 \tag{3.12}$$

so that there is a mean flow down the slope. Finally, the zonal wind is $u = u_g[1 - \cos\lambda z\exp(-\lambda z)]$ so that we have easterlies throughout the atmosphere. It is

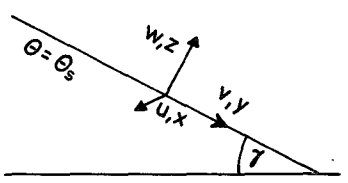

FIG. 2. Coordinate system for the one-dimensional slope wind theory.

somewhat surprising that $v \sim \sin\gamma^{-1}$. This means that the slope winds become infinitely strong for $\gamma \to 0$ since λ remains finite. This is in contrast to the non-rotating case where $\lambda^2 \sim \sin\gamma$ so that v is independent of γ (Prandtl, 1942). Since $\gamma \sim 10^{-3}$ is so small in the interior of Antarctica, one obtains slope winds with $v \sim 100$ m s^{-1} and more for realistic values of the parameters. We arrive at the conclusion drawn already by Lykosov and Gutmann (1972) that (3.8) with $\delta = 0$ is not a suitable equation for our problem. When radiative damping is included (3.8) becomes considerably more cumbersome. However since γ is so small we may assume that $N_0^2 \sin^2\gamma \ll |f|$ and we can then neglect the term $N_0^2 \sin^2\gamma/K^2$ in (3.9). Then it is easy to find the solutions of (3.8). There are six basic functions of the form $\exp(-\alpha_i z)$. We have to choose those decaying with height

$$\alpha_1 = (\delta/K)^{1/2}$$
$$\alpha_2 = (1 + i)\kappa$$
$$\alpha_3 = (1 - i)\kappa \qquad (3.13)$$

where $\kappa^{-1} = (f/2K)^{-1/2}$ is the classical Ekman height. It is straightforward to obtain the temperature profile since the "adiabatic" term $N_0^2 \sin\gamma v/g$ in (3.3) must be neglected. We have

$$\theta = \theta_s \exp(-\alpha_1 z). \qquad (3.14)$$

The profile of the potential temperature is determined through a balance of turbulent heat flux convergence and radiative damping. In contrast to (3.10) the temperature simply decays exponentially with increasing height. The components of velocity are

$$v = KB(\alpha_1^2 \exp(-\alpha_1 z) - [(2\kappa^2 \sin\kappa z + \alpha_1^2 \cos\kappa z) \exp(-\kappa z)] \qquad (3.15)$$

$$u = -Bf\cos\gamma\left[\exp(-\alpha_1 z) - \left(\cos\kappa z - \frac{\alpha_1^2}{2\kappa^2}\sin\kappa z\right)\exp(-\kappa z)\right] \qquad (3.16)$$

with $B = \theta_s g \sin\gamma/\theta_0(f^2\cos^2\gamma + \delta^2)$.

At the ground we find

$$\frac{\partial v}{\partial z} = KB(-\alpha_1^3 - 2\kappa^3 + \alpha_1^2\kappa)$$
$$\frac{\partial u}{\partial z} = -Bf\cos\gamma(-\alpha_1 + \kappa + \alpha_1^2/2\kappa).$$

Since $\delta \ll f$ we have $\alpha_1 < |\alpha_2||\alpha_3|$ and, correspondingly, $\partial v/\partial z > 0$, $\partial u/\partial z < 0$ at $z = 0$. We have downslope winds and easterlies near the ground. Aloft, velocities decay $\sim \exp(-\alpha_1 z)$. There is no geostrophic wind required in order to have a steady state. We have weak southeasterlies aloft. The main point of our analysis is that now both u and $v \sim \sin\gamma$ so that the singularity of the problem is removed. With $\delta = 0$ the adiabatic warming of the descending slope wind had to balance the surface cooling. Because of the small inclination of the slope, enormous wind velocities were required in the rotating case. With $\delta > 0$ this adiabatic effect is no longer important. The only important coupling of the temperature field with the dynamics is through the buoyancy term in (3.2). The complete solution of (3.8) has been evaluated as well. It is not immediately obvious which value to choose for the radiative damping parameter. Since this damping appears to act on the timescale of a few days we choose $\delta = 1/5$ d^{-1}. Then it is found that the roots of the characteristic polynomial are close to (3.13). We show the slope wind, u and θ in Fig. 3. The slope wind has a maximum at a height of about 150 m ($\pi/4\kappa \sim 170$ m). There is weak return flow aloft. In correspondence with (3.16) the zonal wind is easterly throughout the atmosphere and vanishes at great heights. The potential temperature decays exponentially with height in agreement with (3.14). The wind profiles are not very sensitive to the choice of the radiative decay parameter. For example the wind-profiles for $\delta = 1/10$ d^{-1} are rather close to those presented in Fig. 3. They are slightly more sen-

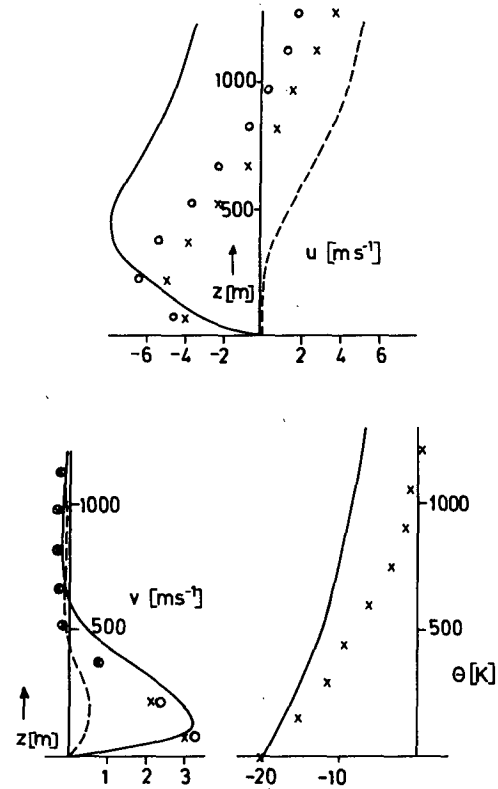

FIG. 3. Wind and temperature profile near the slope. Full lines: solution of (3.8) for $K = 3$ m^2 s^{-1}, $\delta = 1/5$ d^{-1}, $N_0 = 10^{-2}$ s^{-1}; crosses: results from the two-dimensional model at $t = 55$ h for $\hat{\gamma} = 0.006$ K m^{-1}; circles: corresponding linear run; dashed lines: modified slope wind theory with vanishing vertically averaged mass flux above the slope.

sitive to the choice of K. As can be seen from (3.9), the thickness of the slope wind layer increases $\sim K^{1/2}$ just as in the conventional Ekman theory. Even without making detailed comparisons with observations we can conclude that the one-dimensional theory with constant K and radiative damping provides quite a reasonable description of the boundary layer flow. Let us now turn to the numerical integration of the two-dimensional model.

4. Results from the axisymmetric model

We discuss first the results obtained for a lapse rate $\hat{\gamma} = 0.006$ K m^{-1} and $K = 3$ m^2 s^{-1}. At the surface we impose $\theta_s = -20$ K over land and $\theta_s = 0$ to the north of the continent. In Figs. 4 and 5 we present the flow after 55 h of integration. The integration has been started with an atmosphere at rest. The flow does not reach a steady state within these 55 hours but is evolving slowly. The meridional flow component is shown in Fig. 4. We have a shallow layer of downslope winds. Typical values of v in this layer are 2–4 m s^{-1}. The speed increases with distance from the pole and there is maximum speed just above the edge of the continent. The slope wind layer has a thickness of 500 m, i.e., the slope wind layer is not very well resolved in the grid of the model. Above the slope wind layer we have a deep layer of weak return flow. There, typical velocities are $v \sim -0.1$ m s^{-1}. Low temperatures are restricted to the slope wind layer. Note the positive temperature deviations above 4000 m. These must have been induced by the descending air in the thermodynamically direct cell enforced by the cooling at the slopes. At $t = 55$ h there is still a shift of mass towards the north. The mass transport by the slope wind is not completely balanced by the return flow and the difference of the interface height between the northern wall of the domain and the South Pole will increase. It is seen from

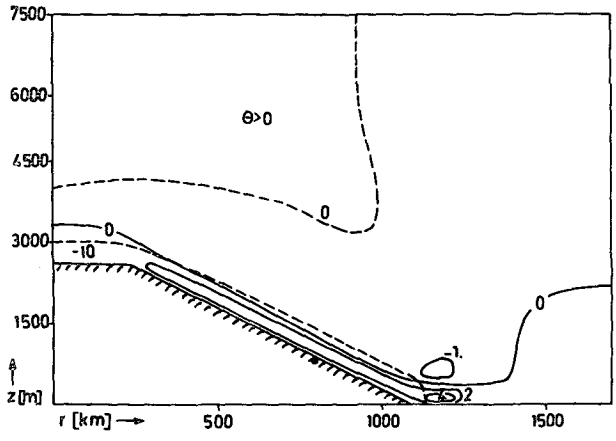

FIG. 4. Meridional velocity v (bold; m s^{-1}) and θ (dashed; K) at $t = 55$ h; $\hat{\gamma} = 6 \times 10^{-3}$ K m^{-1}, $\delta = 1/5$ d^{-1}; $g' = 1$ m s^{-2}, $K = 3$ m^2 s^{-1}. The dot marks the point where the velocity profiles shown in Fig. 3 have been evaluated.

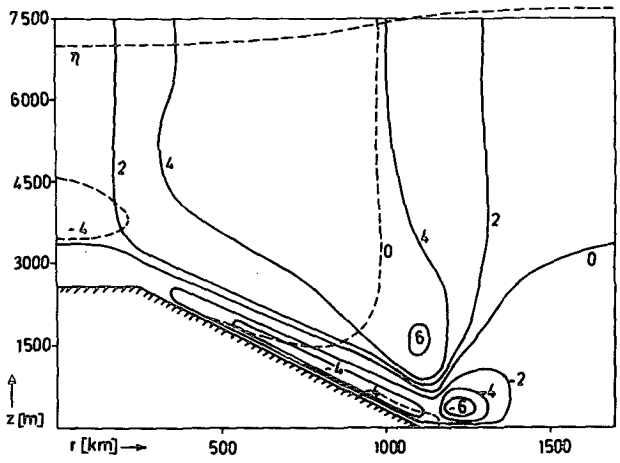

FIG. 5. Zonal velocity u (bold; m s^{-1}), pressure (dashed; mb) and η (dashed; m) at $t = 55$ h; $\hat{\gamma} = 6 \times 10^{-3}$ K m^{-1}; $g' = 1$ m s^{-2}, $K = 3$ m^2 s^{-1}, $\delta = 1/5$ d^{-1}.

Fig. 5 that we now have a height distance of about 500 m between north and south. This is more than $\Delta z = 300$ m. It has to be kept in mind, however, that η enters the problem in (2.3) in conjunction with the parameter g'. By choosing large values of g' we can reduce the amplitude of η considerably. We have rerun the experiment with $g' = 9.81$. It has been found that this change had relatively little impact on the wind profiles but the height difference was then only 70 m at $t = 55$ h. It is certainly not necessary to have a grid system which can follow such small changes of the height of the interface and we feel justified in using this grid even for smaller values of g'. The zonal wind is easterly in the slope wind layer with a maximum of easterlies at the edge. Above the slope wind layer the zonal wind turns westerly with a pronounced maximum at the edge. At the interface we have geostrophic westerlies of about 4 m s^{-1}. The pressure deviation is also presented in Fig. 5. Near the interface the pressure is governed by the height deviation of the interface, i.e., we have high (low) pressure to the north (south). At lower levels the influence of the temperature deviations will be seen. Therefore, we have a minimum of pressure well above the slopes just below the layer of relatively warm air. Closer to the slopes the pressure increases with decreasing height. The largest values of the pressure deviation are found at sea level to the north of Antarctica. Note that we have an increase of pressure down the slope so that the slope wind has to do work against the pressure gradient force.

We want to relate these flow patterns to the one-dimensional theory presented above although we have to bear in mind that no steady state has been reached in the model. In Fig. 3 we show the profiles of u, v, θ as obtained at a grid point about halfway down the slope (see Fig. 4 for exact location) for comparison with the one-dimensional theory. Note that the parameters do have the same values in both cases except for sta-

bility, which is weakly height-dependent in the numerical experiment. The slope wind profiles agree quite well but the agreement of the zonal wind profiles is good only near the ground. Higher up the zonal wind is westerly in the model but easterly according to the one-dimensional theory. The temperature profiles are both exponentially decaying but the model atmosphere is relatively warmer. This is not simply due to the slow approach to equilibrium in time. We have solved the time dependent form of the slope wind Eqs. (3.1)–(3.3) numerically. It has been found that the one-dimensional solution is rather close to the equilibrium after 55 h at least in the lowest 600 m. We can conclude that the one-dimensional theory describes quite well all the profiles close to the ground at least for the first days of flow development. However, the one-dimensional theory fails well above the slope wind layer where it predicts easterlies decaying with height. Of course it is the pressure gradient term in (3.2) which is mainly responsible for this deviation from the one-dimensional theory. For $\delta = 0$ we had an upslope pressure gradient (3.7) and there is no pressure gradient at all with radiative damping included. We have computed the terms of (3.2) in the numerical run at the grid points closest to the ground. We find that the buoyancy term is largest ($\sim 1.7 \times 10^{-3}$ m s^{-2}). The pressure gradient term and the Coriolis term are of the same order of magnitude ($\sim 0.7 \times 10^{-3}$) and are both opposed to the buoyancy term. Vertical diffusion of momentum is less important at the lowest grid point (0.5×10^{-4}). This analysis shows clearly that the horizontal pressure gradient term which is not handled properly in the one-dimensional theory is indeed important. On the other hand, advection of momentum is unimportant ($\sim 10^{-6}$). To demonstrate further the overall linear character of the flow fields shown in Figs. 4 and 5 we have rerun the experiment with all advective terms neglected so that $d/dt = \partial/\partial t$ in (2.1), (2.2), (2.4), and (2.6). The resulting zonal wind is shown in Fig. 6. The similarity to Fig. 5 is obvious. Note in particular that the geostrophic wind at the free surface is almost exactly the same in both runs. The easterlies in the slope wind layer are more intense in the linear run as are the westerlies above the edge of the continent. In Fig. 3 we give a profile of the slope wind as obtained in the linear run. The agreement with the nonlinear profile is almost perfect, but the easterlies are somewhat too intense. A few more experiments have been conducted in order to see how the circulation in the two-dimensional domain depends on the parameters. An increase (decrease) of the lapse rate to $\hat{\gamma} = 0.009$ K m^{-1} (0.003) had surprisingly little effect. Increasing the coefficient K is equivalent to thickening the slope wind layer. With $K = 10$ m^2 s^{-1} the slope wind layer has a depth of about 750 m as compared to 450 m in Fig. 3. We have also run a winter case where it is assumed that the ocean is ice-covered and where $\theta_s = -20$ K is the same at all

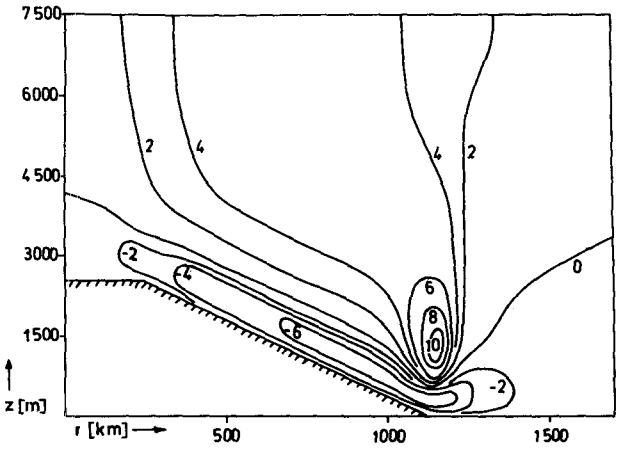

FIG. 6. Zonal velocity u (bold; m s^{-1}) at $t = 55$ h in the linear run corresponding to that shown in Fig. 5.

bottom grid points. The implementation of this surface temperature distribution results in a slightly reduced slope wind. In particular there is no maximum of v at the edge of Antarctica. As for the zonal wind, the maximum of the easterlies is now above the slope (Fig. 7). The large vertical shear at the edge seen in Fig. 5 is now missing. This is not surprising. In the standard experiment we had a jump of the surface temperature which induces a cooling at the edge. Even without the slope such a jump would produce a strong circulation similar to that seen in Fig. 5 near the edge. If we remove the jump we also remove the circulation created by it. A change in the position of the northern wall of the domain had little effect on the circulation when it was moved by 250 km toward the south. An experiment with $\delta = 0$ resulted in flow patterns which were slightly more intense than those shown in Figs. 4 and 5. Note that the one-dimensional slope wind equations (3.1)–(3.3) yield quite reasonable profiles for quite a while if integrated in time with $\delta = 0$. It is only the equilibrium state which is unrealistic. Correspondingly we need not be surprised that the two-dimensional model yields reasonable flow patterns with $\delta = 0$ at $t = 55$ h. The flow is not very sensitive to alterations of the mean flow height H_0 within reasonable limits.

5. Discussion

We have extended the time of integration for most runs until $t = 111$ h. This resulted in a slight weakening of the slope wind and a further increase of the pressure gradient along the slope. Clearly no steady state had been reached by that time. The standard experiment could not be continued beyond that time since first signs of numerical instability appeared near the South Pole. The experiment with $\hat{\gamma} = 0.003$ K m^{-1} and the linear experiment have been advanced further in time but it was not possible to achieve a steady state within

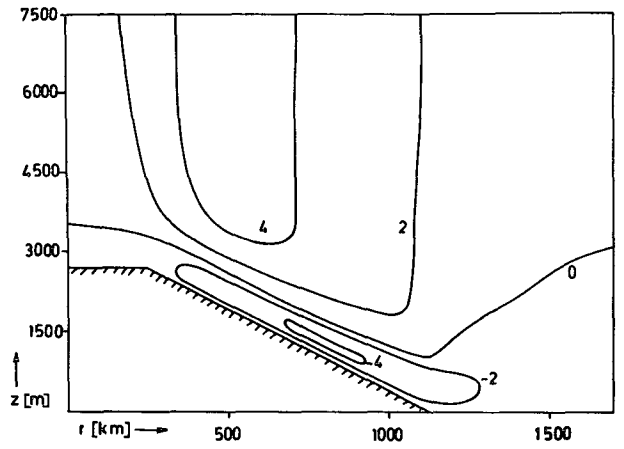

FIG. 7. Zonal velocity u (m s^{-1}) at t = 55 h in the run where $\theta_s = -20$ K at all grid points of the lower boundary.

two more days of integration. This leads us to ask why we cannot attain a steady state within reasonable times of integration. A partial answer can be given by looking at the diffusive time scales involved. The air in the flow domain must adjust to the low surface temperature. This is done mainly through the circulation set up above the slope, but eddy diffusion of temperature plays a role as well. The corresponding time scale $H_0^2/K \sim 3 \times 10^7$ s is rather long. There is, however, another more rapid process linked to the balance of angular momentum in the model. As is well known we may rewrite the first equation of motion in the form

$$\frac{dM}{dt} = K\frac{\partial^2 M}{\partial z^2} \tag{4.1}$$

where

$$M = ru + fr^2/2. \tag{4.2}$$

Now if we integrate (4.1) over the flow domain and if we assume steady-state conditions, we find

$$0 = \int_{\text{bottom}} K\frac{\partial}{\partial z}(ru)dr \tag{4.3}$$

since we have no stress at the interface and since the terms on the left hand of (4.1) cannot contribute to the budget because there is no transport of angular momentum through the solid walls of the flow domain. Note that (4.3) is not satisfied in the one-dimensional theories proposed so far. In these theories one has a nonvanishing mean flow $\int_0^\infty vdz$ down the slope [see (3.12), for example]. This mean flow provides a Coriolis-torque which can balance the surface stress term. In the two-dimensional model (4.3) must be satisfied if a steady state is to be attained. However, since downward slope winds go with easterlies we have a source of westerly momentum at the slope which would have to be balanced by a sink of westerly momentum over the ocean. This sink could be provided by westerlies over the ocean but our model does not contain a mechanism for maintaining strong westerlies over the ocean. We conclude that the only way to reach a steady state in our model would be to almost suppress the slope winds. That is possible only if the inclination of the interface becomes so large that the corresponding pressure gradient is able to stop the flow down slope so as to make the slope winds almost disappear. One may ask how the atmosphere copes with this situation. After all, we observe surface easterlies in Antarctica and, correspondingly, the slope of Antarctica is a source of westerly momentum. The answer appears to be that the three-dimensional synoptic-scale eddies over Antarctica export the westerly momentum gained at the surface towards the north. The maps prepared by Oort (1983) show this transport quite clearly. Moreover, an order of magnitude argument shows that the gain of westerly momentum in the model during the first days of numerical integration equals roughly the observed export in the atmosphere. However, since angular momentum cannot be exported in the model the long-term flow evolution must become increasingly unrealistic. We can accelerate this evolution by replacing the free surface on top by a rigid lid. The pressure at the rigid lid is computed by requiring that there is no net radial mass flux. This way the pressure field can be built up instantaneously whereas relatively slow mass transports were required to influence the height of the free surface. Indeed the speed of the slope winds is reduced faster if a lid is placed on top. For the case of an ice-covered ocean, for example, we obtain v = 1.3 m s^{-1} after 111 h at the grid point shown in Fig. 4 when the rigid-lid condition is implemented as compared to v = 1.9 m s^{-1} for the free surface case. Now if our argumentation is correct, there should be virtually no slowing down for the nonrotating case. If $f = 0$ we have $u = 0$ for all time and, correspondingly, there are no problems with the angular momentum balance. Indeed, v = 5.2 m s^{-1} at t = 111 h for the nonrotating case with a rigid lid.

It is tempting to speculate about the flow profiles one would obtain in our model if a steady state would be attained after a sufficiently long time of integration. We do this by modifying the one-dimensional theory presented in Section 3. If a steady state in a closed domain is to be achieved there should be no mean transport of mass down the slope. Therefore we have to require

$$\int_0^\infty vdz = 0 \tag{4.4}$$

in addition to satisfying (3.1)–(3.3). We determine the north–south pressure gradient term $fu_g \cos\gamma$ in (3.2) so that (4.4) can be satisfied. After all, we have seen in the analysis of the boundary layer in the numerical

runs that this term is important. There is no problem in solving the set of equations with the new boundary condition $u = 0$ at $z = 0$ and $u = u_g$ at $z = 00$. We shall discuss first the case where the adiabatic term $N_0^2 \sin\gamma v/g$ is neglected in (3.3). Then $\theta = \theta_s \exp(-\alpha_1 z)$ as in Section 3 (3.14) and it is straightforward to solve the problem. One finds to a good approximation:

$$u_y = Bf\cos\gamma. \tag{4.5}$$

Since B and f are negative we now obtain westerlies aloft. The approximate wind profiles are exactly the same as (3.15), (3.16) except that a conventional Ekman-spiral induced by (4.5) must be added. In Fig. 3 we show the exact solution of the problem. Near the surface we have now very weak westerlies. However, since $\partial u/\partial z = 0 = \partial^2 u/\partial z^2$ at the ground these westerlies are extremely weak. Note also that the slope winds are now quite weak. Aloft we have strong westerlies and a weak return flow. Obviously, this solution is unrealistic near the ground but realistic aloft. This supports our view that the long-term evolution of the two-dimensional flow will lead to unrealistic flow patterns. However since this evolution appears to be rather slow it is meaningful to compare the quasi-stationary two-dimensional flow obtained after a few days to that observed in Antarctica. In the slope wind layer, most wind measurements have been made close to the ground whereas the lowest level of the computed wind is about 75 m above the ground. So a strict comparison with observations is not possible. Observed wind velocities near the ground are of the order ~ 5 m s^{-1} (Schwerdtfeger, 1970) which agrees reasonably well with what we find in the model. The observed surface winds form an angle of about forty five degrees (Schwerdtfeger, 1970) and more (Parish, 1984) with the slope direction again in reasonably good agreement with the model results and those given by the one-dimensional theory. The temperature profile over the slopes of the interior is exponentially shaped as is found in the model. It is, however, a disadvantage of the model used that the boundary layer thickness is specified *a priori* through the choice of the diffusion coefficient K. In more advanced models of the boundary over gently sloping terrain the height of the boundary layer evolves according to circumstances (Lykosov and Gutman, 1972; Sorbjan, 1984). All in all, we feel that the gross features of the Antarctic slope wind layer are represented reasonably well in the model. Higher up we observe westerlies throughout the year and correspondingly, a low centered near the South Pole. According to Oort (1982) we have westerlies of more than 5 m s^{-1} in the upper troposphere in winter. The wind intensity is less than 5 m s^{-1} in summer. Our model results suggest that the slope wind circulation induced by the cooling at the slopes would be sufficient to induce zonal winds of the observed order of magnitude.

The two-dimensional model predicts strong vertical shears and a westerly jet above the edge of the continent (Fig. 5). There is no observational evidence in support of this model result. However, we learn from Fig. 7 that this jet is due to the prescribed jump of the surface temperature at the edge. This strong contrast of the heating rates is certainly not very realistic nor are the flow patterns caused by it. In reality the slope tends to be much steeper near the coast than is prescribed in our model. Very intense katabatic winds are observed there (Schwerdtfeger, 1970), a feature which is of course missing in our simulation.

One would also like to compare the axisymmetric model results to GCM simulations. One gets the impression, however, that the flow simulations by various groups so far have not converged to the point where a relatively clear picture of the Antarctic circulation in a typical GCM emerges (see JOC, 1979). Model results still differ widely. It is interesting that the winter flow in the Oregon State University two-level model (Schlesinger and Gates, 1979) is similar to that given by the axisymmetric model. There are surface easterlies, westerlies aloft (except very close to the pole) and downward motion over Antarctica. Of course, the slope wind circulation cannot be resolved in a two-level model.

In conclusion we may state that there is a reasonably good qualitative agreement of model results and observations not only in the boundary layer but also well above the slope. We have to conclude that the slope wind regime influences the tropospheric circulation of Antarctica. This does not come as a surprise since a heat sink of horizontal scale R will set up a circulation of vertical extent $H \sim Rf/N_0 \sim H_0$ (e.g., Egger, 1983). Nevertheless it is surprising that the westerlies induced by the cooling at the slopes are so strong. We have, however, to keep in mind that part of this westerly momentum would have been transported to the north if three-dimensional eddies were admitted in our model. Data studies (Oort, 1984) show clearly that eddies play an important role in Antarctica. This view is supported by the numerical experiments of Mechoso (1981). We have to conclude, therefore, that running the axisymmetric model in combination with studying one-dimensional models is clearly helpful for an understanding of the circulation of Antarctica. To make further progress, the effects of three-dimensional eddies have to be taken into account.

REFERENCES

Ball, F. K., 1960: Winds on the ice slopes of Antarctica. *Antarctic Meteorology: Proc. Symp.*, Melbourne, Pergamon, 9–16.

Egger, J., 1983: Topographic forcing. *Mesoscale Meteorology: Theories, Observations and Models*, D. Lilly and T. Gal-Chen, Eds., Reidel, 321–337.

Hermann, G. F., and W. T. Johnson, 1980: Artic and Antarctic climatology of a GLAS general circulation model. *Mon. Wea. Rev.*, **108**, 1974–1991.

JOC, 1979: Report of the JOC study conference on climate models: Performance, intercomparison and sensitivity studies. Part I. GARP Publ. Ser. No. 22, WMO, 606 pp.

Kasahara, A., 1974: Various vertical coordinate systems used for numerical weather prediction. *Mon. Wea. Rev.*, **102,** 509–522.

Lykosov, V. N., and L. N. Gutman, 1972: Turbulent boundary layer above a sloping underlying surface. *Izv. Acad. Sci. USSR, Atmos. Ocean. Phys.*, **8,** 799–809.

Mather, K. B., and G. S. Miller, 1967: Notes on topographic factors affecting the surface wind in Antarctica, with special reference to katabatic winds, and bibliography. Geophys. Inst. Rep. UAGR-189, University of Alaska, Fairbanks, 125 pp.

Mechoso, C., 1981: The atmospheric circulation around Antarctica: Linear stability and finite amplitude interactions with migrations cyclones. *J. Atmos. Sci.*, **37,** 2209–2233.

Oort, A., 1983: *Global Atmospheric Circulation Statistics, 1958–1979.* NOAA Prof. Pap. 14, 80 pp.

Parish, T., 1984: A numerical study of strong katabatic winds over Antarctica. *Mon. Wea. Rev.*, **112,** 545–554.

Prandtl, L., 1942: Strömungslehre. Vieweg & Sohn; Braunschweig.

Roache, P., 1976: *Computational Fluid Dynamics,* Hermosa Publications, 73–75.

Schlesinger, M., and W. Gates, 1979: Performance of the Oregon State University two-level atmospheric general circulation model, JOC, p. 139–207.

Schwertfeger, W., 1970: The climate of the Antarctic, *World Survey of Climatology,* Vol. 14, H. E. Landsberg, Ed., Elsevier, 253–355.

Sorbjan, Z., 1984: A model study of the stably stratified steady-state atmospheric boundary layer over a slightly inclined terrain. *J. Atmos. Sci.*, **41,** 1863–1873.

van Loon, H., 1972: Wind in the Southern Hemisphere. *Meteorology of the Southern Hemisphere, Meteor. Monogr.*, No. 14, Amer. Meteor. Soc., 87–99.